

Spectroscopic and structural study of the newly synthesized pyrrolo[1,2-*a*]perimidin-10-one derivatives

İrfan Koca^{*1}, Mustafa Büyükata², Salih Cınaklı², Yunus Oruç¹
and Şevket Hakan Üngören¹

¹Department of Chemistry, Faculty of Art & Sciences, Bozok University, TR-66200 Yozgat, Türkiye

²Department of Physics, Faculty of Art & Sciences, Bozok University, TR-66200 Yozgat, Türkiye

(Received October, 2016; Revised November 11, 2016; Accepted November 27, 2016)

Abstract: In this study, pyrrolo[1,2-*a*]perimidin-10-one compounds were synthesized by the reaction of maleic anhydride with heterocyclic ketene aminals (HKAs) containing perimidine moiety. The structures of these novel compounds were confirmed by IR, ¹H NMR, ¹³C NMR, UV and elemental analysis. In order to develop a more understanding of the energetic and structural properties of pyrrolo[1,2-*a*]perimidin-10-ones, a series of theoretical calculations were performed. Their geometries have been optimized by using Hartree-Fock and Density Functional Theory. The structures of possible conformations have been examined to predict lower-lying energy structure of the title molecule. Structural parameters and energetics, such as HOMO and LUMO energies, were analyzed comparing the structural isomers.

Keywords: Perimidine; Pyrrolo[1,2-*a*]perimidine; HF; DFT. © 2016 ACG Publications. All rights reserved.

1. Introduction

Perimidines, which can also be called as 1*H*-benzo[*d,e*]quinazoline, are tricyclic compounds containing pyrimidine and naphthalene moiety. Perimidine derivatives with wide range area of applications have been used as dyes,¹ antioxidant stabilizers,² photochromic compounds,³ fluorescent molecular sensors⁴ and catalyst.⁵ Their biological activity has also been examined, for antifungal, antimicrobial, anticancer and antiulcer agents.⁶⁻⁸ The applications of the considered molecules are in close relations with their various chemical and physical properties based on their structures and energetics. Even though there are experimental studies on similar perimidine derivatives,⁹⁻¹¹ the needs for studying such kind of molecules are still continuing in experimental and especially in theoretical area. The determination of structural stability and energetically lower-lying tautomers is still a task in investigations of chemical and physical properties of perimidine derivatives, which are important for their potential applications.

As a part of the current experimental studies on the synthesis of heterocyclic fused perimidine compounds such as isoindolo[2,1-*a*]perimidines⁹ and pyrrolo[1,2-*a*]perimidin-10-ones,¹⁰ we report herein preparation of novel pyrrolo[1,2-*a*] perimidin-10-ones by the reaction of maleic anhydride with

* Corresponding Author: E-mail: i_koca@yahoo.com; Tel: + 90 354 242 1021; Fax: + 90 354 242 1022

heterocyclic ketene amins (HKAs) containing perimidine moiety. The structures of the synthesized compounds were characterized by IR, ^1H NMR, ^{13}C NMR and elemental analysis.

As a complementary investigation, the structures of considered title molecules have been optimized by using ab initio Hartree-Fock (HF) and Density Functional Theory (DFT). Their structural and energetic properties have been determined and compared with the experimental findings. HF and DFT have been performed with 6-311++G(d,p) basis set, which is an efficient level of theory for various molecular systems.¹²⁻¹⁴

2. Experimental

2.1. General remarks

Melting points are uncorrected and recorded on Electrothermal 9200 digital melting point apparatus. Leco-932 CHNS-O Elemental Analyser was used for elemental analysis. FTIR absorption spectra (4000–400 cm^{-1}) were measured using the ATR technique with Perkin Elmer Spectrum Two Model FT-IR Spectrophotometer. The ^1H and ^{13}C NMR spectra were measured with Bruker Avance III 400 MHz spectrometer using DMSO- d_6 solvent. UV-Vis spectra was recorded in the region 200–550 nm using a Hach Lange DR 5000 Model UV-Vis spectrometer. The reactions were monitored by TLC (Silica gel, aluminum sheets 60 F254, Merck). Solvents were dried by refluxing with the appropriate drying agents and distilled before using.

2.2. General procedure for the synthesis of pyrrolo[1,2-*a*]perimidin-10-ones

HKAs (1mmol) was added to a stirred solution of maleic anhydride (1mmol) in acetonitrile (20 mL) and the mixture was heated at reflux for 2hrs. The resulting solid was collected. The crude product washed with hot toluene and ethyl acetate for purification and dried (P_2O_5).

2.2.1. (8-acetyl-10-oxo-9,10-dihydro-7H-pyrrolo[1,2-*a*]perimidin-9-yl)acetic acid (**2a**)

Brown crystals, (in CHCl_3 , $R_f = 0.48$), yield: 81%; mp 224-226 °C. FT-IR (ATR) ν/cm^{-1} 3165 (NH), 1759, 1707, 1643 (C=O), 1618-1438 (C=C, C=N); ^1H NMR (400 MHz, DMSO- d_6): δ 12.42, (s, 1H, OH), 11.45 (s, 1H, NH), 8.38-7.26 (m, 6H, Ar-H), 3.95 (dd, J 5.4, 3.6 Hz, CH, enamine form), 3.01 (dd, J 16.6, 3.5 Hz, 1H, Ha, CH_2 , A part of ABX system), 2.91 (dd, J 16.6, 5.6 Hz, 1H, Hb, CH_2 , B part of ABX system), 2.08 (s, 3H, CH_3) ppm; ^{13}C NMR (100 MHz, DMSO- d_6): δ 188.3, 175.4, 170.9 (C=O), 172.2 (NH-C=C), 134.0, 134.0, 132.2, 130.4, 128.4, 127.9, 123.6, 121.3, 114.4, 110.3, 109.7, 91.1 (C=C, C=N), 41.6 (CH), 36.0 (CH_2), 27.0 (CH_3) ppm. Anal. Calcd for $\text{C}_{18}\text{H}_{14}\text{N}_2\text{O}_4$ (m/z : 322.31): C, 67.07; H, 4.38; N, 8.69. Found: C, 66.77; H, 4.23; N, 8.66%.

2.2.2. (8-benzoyl-10-oxo-9,10-dihydro-7H-pyrrolo[1,2-*a*]perimidin-9-yl)acetic acid (**2b**)

Brown crystals, (in CHCl_3 , $R_f = 0.45$), yield: 82%; mp 235-236 °C. FT-IR (ATR) ν/cm^{-1} 3154 (NH), 1765, 1709, 1640 (C=O), 1611-1438 (C=C, C=N); ^1H NMR (400 MHz, DMSO- d_6): δ 12.24 (s, 1H, OH), 12.12 (s, 1H, NH), 8.40-7.35 (m, 11H, Ar-H), 5.18 (d, J 5.4 Hz, CH, imine form), 4.36 (t, J 4.2 Hz, CH, enamine form), 2.93 (broad d, CH, imine form), 2.73 (dd, J 16.9, 3.4 Hz, 1H, Ha, CH_2 , A part of ABX system), 2.13 (dd, J 16.9, 5.2 Hz, 1H, Hb, CH_2 , B part of ABX system) ppm; ^{13}C NMR (100 MHz, DMSO- d_6): δ 183.8, 175.5, 152.8 (C=O), 171.8 (NH-C=C), 140.3, 134.1, 132.2, 130.9, 130.4, 130.1, 129.2, 129.0, 128.8, 128.5, 128.0, 127.2, 123.7, 121.7, 119.0, 115.0, 110.8, 109.8, 90.9 (C=C, C=N), 41.8 (CH), 34.8 (CH_2) ppm. Anal. Calcd for $\text{C}_{23}\text{H}_{16}\text{N}_2\text{O}_4$ (m/z : 384.38): C, 71.87; H, 4.20; N, 7.29. Found: C, 71.47; H, 4.19; N, 7.19%.

2.2.3. [8-(4-methoxybenzoyl)-10-oxo-9,10-dihydro-7H-pyrrolo[1,2-*a*]perimidin-9-yl]acetic acid (**2c**)

Brown crystals, (in CHCl_3 , $R_f = 0.44$), yield: 86%; mp 235-236 °C. FT-IR (ATR) ν/cm^{-1} 3202 (NH), 1750, 1729, 1641 (C=O), 1597-1443 (C=C, C=N) cm^{-1} ; ^1H NMR (400 MHz, DMSO- d_6): δ 12.22 (s, 1H, OH), 8.40-7.01 (m, 10H, Ar-H), 5.12 (d, J 5.2 Hz, CH, imine form), 4.40 (t, J 3.9 Hz, CH, enamine form), 3.89, 3.83 (2 \times s, 3H, OCH_3), 2.91 (d, J 6.1 Hz, CH, imine form), 2.79 (dd, J 16.7, 3.2 Hz, 1H, Ha, CH_2 , A part of ABX system), 2.30 (dd, J 16.9, 5.0 Hz, 1H, Hb, CH_2 , B part of ABX system) ppm; ^{13}C NMR (100 MHz, DMSO- d_6): δ 194.5, 182.6, 175.6, 175.6, 171.8 (C=O), 172.9

(NH-C=C), 164.3, 161.5, 156.1, 152.7, 134.4, 134.1, 132.6, 132.4, 132.4, 130.5, 129.4, 128.8, 128.5, 128.0, 127.9, 123.9, 123.7, 123.6, 121.6, 118.9, 115.0, 114.5, 114.2, 110.7, 109.8, 109.0, 90.7 (C=C, C=N, aromatic), 56.2, 55.8 (OCH₃), 49.8 (CH, imine form), 41.9 (CH, enamine form), 40.9 (CH, imine form), 34.8, 34.5 (CH₂) ppm. Anal. Calcd for C₂₄H₁₈N₂O₅ (*m/z*: 414.41): C, 69.56; H, 4.38; N, 6.76. Found: C, 69.53; H, 4.12; N, 6.35%.

2.2.4. [8-(3,4-dimethoxybenzoyl)-10-oxo-9,10-dihydro-7H-pyrrolo[1,2-*a*]perimidin-9-yl]acetic acid (**2d**)

Brown crystals, (in CHCl₃, R_f = 0.38), yield: 83%; mp 222-223 °C. FT-IR (ATR) v/cm⁻¹ 3151 (NH, OH), 1764, 1726, 1641 (C=O), 1610-1446 C=C, C=N; ¹H NMR (400 MHz, DMSO-*d*₆): δ 12.27 (s, 1H, OH), 8.40-6.87 (m, 9H, Ar-H), 5.13(d, *J* 4.9 Hz, CH, imine form), 4.45 (broad *t*, CH, enamine form), 3.90, 3.85, 3.83, 3.81 (4 × s, 6H, OCH₃), 2.91 (d, *J* 6.1 Hz, CH, imine form), 2.78 (dd, *J* 17.0, 3.6 Hz, 1H, Ha, CH₂, A part of ABX system), 2.34 (dd, *J* 17.0, 5.3 Hz, 1H, Hb, CH₂, B part of ABX system) ppm; ¹³C NMR (100 MHz, DMSO-*d*₆): δ 195.4, 182.7, 175.6, 175.3, 171.9, 156.1, (C=O), 172.9 NH-C=C), 154.3, 152.7, 151.3, 149.0, 148.9, 139.8, 134.4, 134.1, 132.5, 132.4, 132.2, 130.5, 128.8, 128.5, 128.0, 127.9, 125.6, 123.9, 123.7, 123.7, 121.6, 120.9, 118.9, 115.0, 111.8, 111.6, 111.4, 110.8, 110.7, 109.8, 109.0, 90.7 (C=C, C=N, aromatic), 56.4, 56.1, 56.0, 56.0 (2 × OCH₃), 49.8 (CH, imine form) 42.0 (CH), 34.8, 34.6 (CH₂) ppm. Anal. Calcd for C₂₅H₂₀N₂O₆ (*m/z*: 444.44): C, 67.56; H, 4.54; N, 6.30. Found: C, 67.84; H, 4.42; N, 6.08%.

2.4. Computational details

The optimized molecular structures and vibrational frequencies for the pyrrolo[1,2-*a*]perimidin-10-one molecules have been obtained by using ab-initio HF and DFT (B3LYP) methods with 6-311++G(d,p) basis set. Their total energies, with and without Zero-Point Energy (ZPE) corrections have been computed. HOMO and LUMO have been determined to predict HOMO-LUMO energy gap values. For all molecules, the geometry optimizations performed with the same basis set for both of the methods. There is no geometry restriction for the structural parameters. The selected initial coordinates of the atoms in the molecules were totally free. Therefore, whole systems are in fully optimized procedure over the potential energy surface for each case. After getting the optimized geometry, stable in the potential energy well, it is recalculated for single point energy and frequency calculations with the same selected method. All computational analyses have been performed on a personal computer using the Gaussian 03 program package¹⁵ and Chemcraft molecular visualization program.¹⁶ The scale factors, 0.9051 and 0.9614, were used for calculated frequencies of HF and B3LYP, respectively.¹⁷ The considered chemical and physical quantities are valuable to investigate the stability of the compounds and to compare with experimental findings.

3. Results and Discussion

3.1. Characterization of pyrrolo[1,2-*a*]perimidin-10-ones (**2a-d**)

The synthesis of pyrroloperimidine compounds were accomplished as described in Figure 1. Our previous studies were based on heterocyclic ketene aminals including perimidine moiety which are used as starting material (**1a-d**)^{9,10}. Hence, we selected the considered compound as starting materials which are the four valuable substituents **a-d**.

Under reflux conditions, in acetonitrile solution of HKAs and maleic anhydride led to the formation of pyrrolo[1,2-*a*]perimidin-10-one linked acetic acids in good yields. The final product was characterized by elemental analyses, IR, ¹H NMR, ¹³C NMR techniques.

Considering the structure of the target compounds, it is seen that there are two tautomeric structures, namely enamine (**A**) and imine (**B**). When the ¹H NMR spectra of **2a-d**, recorded in DMSO-*d*₆ at room temperature, were investigated, the signals of both tautomers were observed, except **2a**. Compound **2a** is almost all in the form of the enamine form. The enamine form is found more than imine form for the other compounds. According to ¹H NMR spectra of **2a-d**, we say that the imine forms of **2a-d** are approximately 0, 17, 39 and 45% in the equilibrium of imine-enamine forms,

Table 1. Some resonances of carbons of compound **2c**

	ppm Enamine forms	ppm Imine Forms
Aroyl	182.6	194.5
Carboxylic acid	175.6	175.4
Amide C=O	171.8	157.0
HN-C=C	90.7	----
Methoxy	55.8	56.2
CH	----	49.8
CH	41.9	40.9
CH ₂	34.8	34.5

In the ¹H NMR spectra of **2c** (Figure 3), OH signal was observed at δ 12.22 ppm. The aromatic protons of the **2c** gave multiplet in the range of 8.40-7.01 ppm. The signal of methine proton (the hydrogen bonded to the asymmetric carbon at the pyrrole ring) in the enamine form was showed up at 4.40 ppm as a triplet. The methylene protons attached to an asymmetric center of a pyrrole ring showed the signals of ABX system as four lines. The signals of these diastereotopic protons were clearly revealed the proposed pyrrole structure. The observed signal at 5.12 ppm belongs to methine group in imine form. And also the signal of other methine proton in imine form observed at 2.91 ppm. Two singlet arised at 3.89 and 3.83 ppm due to methoxy protons.

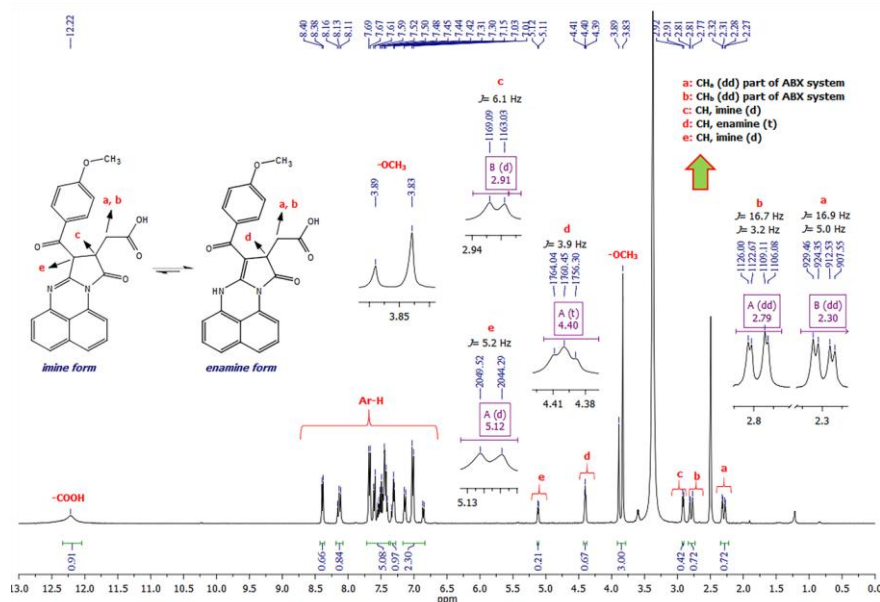
**Figure 3.** ¹H NMR spectra of compound **2c**

Figure 4 demonstrates the geometries of **2a-2d** for both tautomers **A** and **B**, predicted by using B3LYP/6-311++g(d,p) level theory. The geometries determined with HF are also the same as the predicted structures with B3LYP. Their energetic quantities of total energies and Highest Occupied Molecular Orbital (HOMO) and Lowest Unoccupied Molecular Orbital (LUMO) energy gaps (gap_{HL}) for the considered molecules are tabulated in Table 2 for **2a-2d** for both **A** and **B** tautomers. The total energies, with and without ZPE corrections, of tautomer **A** calculated with B3LYP are lower than

those ones for tautomer **B** for all compounds, **2a** to **2d**. The differences between A and B for total energy are 0.12 eV, -0.013 eV, 0.027 eV, 0.135 eV for **2a-2d** in HF and -0.159 eV, -0.286 eV, -0.243 eV, -0.133 eV for **2a-2d** in B3LYP. This means that tautomer **A** is energetically more stable than tautomer **B**. Therefore, the number of the compound, energetically more stable tautomer **A**, may be expected to be larger than the number of **B** compound in the experimental environment. This result clearly confirms the experimental findings. With respect to this confirmation, these particular structures without searching any conformational analysis were investigated through optimization procedure without geometry restrictions that the molecules can prefer any lower-lying energy position on the potential energy surfaces around the initial configuration. However, the total energies calculated with HF do not confirm this result for all compounds, except **2b**.

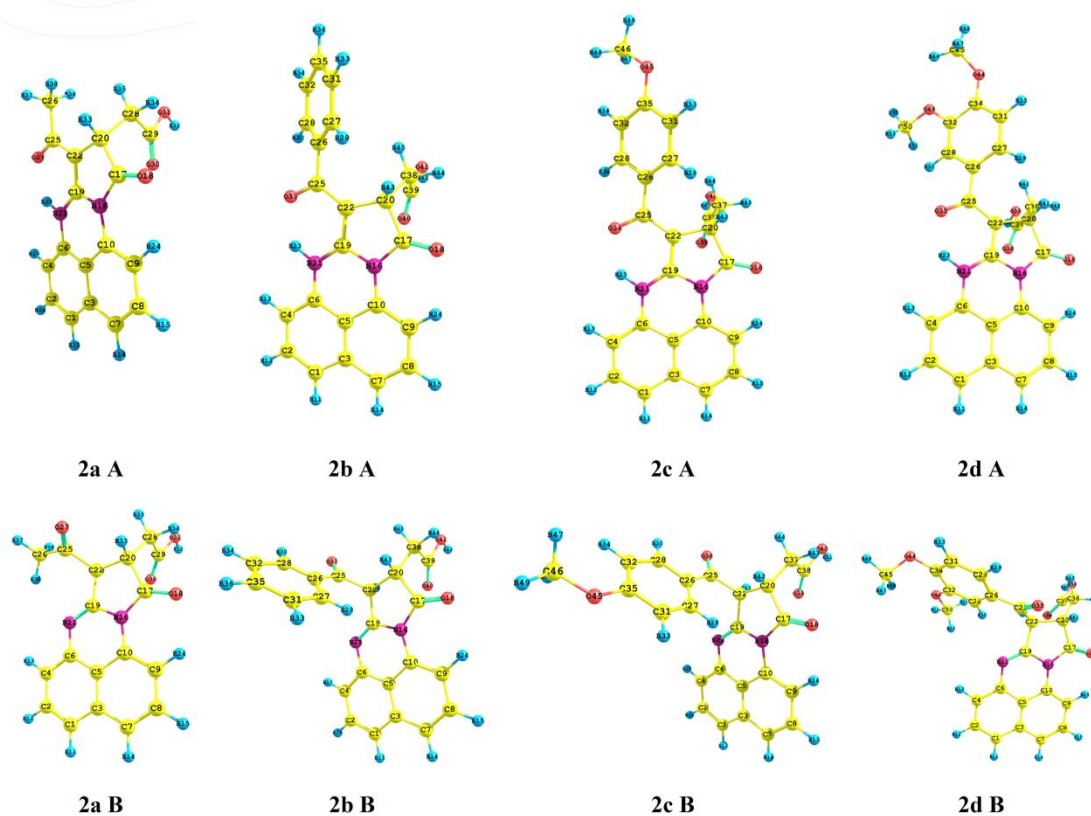


Figure 4. Geometries of **A** and **B** for **2a-2d** obtained by B3LYP/6-311++g(d,p)

Theoretically all structures for the title compounds can be optimized for analyzing structural and energetic properties. The determined structural parameters are given in supplementary material. The selected theories, HF and B3LYP, have confirmed the structural stability of the tautomeric forms of these compounds. It is found that the lower-lying energy structure of tautomer **A** is more stable than tautomer **B** with respect to DFT/B3LYP results. On the other hand, enamine form (tautomer **A**) is more than imine form (tautomer **B**) according to the experimental results. Hence, it can be expected that the total energy of enamine form (tautomer **A**) should be energetically more stable than imine form (tautomer **B**). However, HF does not confirm the same results. As a result, B3LYP is more useful for this kind of compounds, instead of HF, since B3LYP considers the electronic interactions more precisely than HF for most of the molecular systems.¹²⁻¹⁴ On the other hand, HOMO-LUMO energy gaps calculated with HF and B3LYP are larger in tautomer **A** than **B**. As a chemical system, tautomer **A** is the lower-lying energy state of the particular compounds and its chemical equilibrium with its environment, i.e. its in dynamic equilibrium and its particular form is conserved. Tautomer **A** is chemically more stable than tautomer **B** for all compounds, **2a-2d** since the energy of HOMO-LUMO

gap of the change from tautomer **A** to tautomer **B** is positive. It means that tautomer **A** should be more than tautomer **B** in the product of **2a-2d**. These results also confirm the experimental results with the respect to the large abundance of tautomer **A**.

Table 2. Energies and HOMO-LUMO gap (gap_{HL}) of molecules **2 (a, b, c and d) A and B** (all values are in eV)

		Energy (E)		Energy + Zero Point Energy (E+ZPE)		Zero Point Energy (ZPE)		gap_{HL}	
		HF	B3LYP	HF	B3LYP	HF	B3LYP	HF	B3LYP
2a	A	-29891.083	-30071.696	-29882.600	-30063.805	8.483	7.891	3.060	2.954
	B	-29891.203	-30071.537	-29882.723	-30063.654	8.480	7.882	3.047	2.887
2b	A	-35076.150	-35290.312	-35066.121	-35280.971	10.029	9.341	2.939	2.761
	B	-35076.137	-35290.026	-35066.103	-35280.687	10.035	9.339	2.676	2.490
2c	A	-38175.873	-38407.581	-38164.894	-38397.364	10.978	10.217	3.013	2.872
	B	-38175.900	-38407.338	-38164.917	-38397.123	10.983	10.216	2.989	2.797
2d	A	-41275.407	-41524.630	-41263.490	-41513.540	11.916	11.090	3.012	2.839
	B	-41275.542	-41524.497	-41263.620	-41513.417	11.922	11.080	2.881	2.696

The graphs given in Figure 5 illustrates the HOMO-LUMO energy gap values of tautomer **A** and tautomer **B** determined with HF and B3LYP as functions of the substituent additions from methyl to aromatic groups, **2a-2d**, respectively. The values for tautomer **B** are lower than those for tautomer **A** for all molecules according to the both methods. **2b** has the lowest gap_{HL} value with respect to the other compounds for both tautomers **A** and **B** with both methods. The HOMO and LUMO clouds of tautomers **A** and **B** of compounds, **2c**, are given in Figure 6. The electronic densities for HOMO are mainly observed on the pyrrolo perimidine parts of the molecules. In spite of the changes in the attached substituents from **2a** to **2d**, electronic saturations almost keep their shape and located over the pyrrolo perimidine parts of the molecules for HOMO orbitals. This is relatively more symmetric on these parts of tautomer **B**. LUMO clouds are more dominant on and around the attached substituents. The differences between tautomer **A** and **B** for HOMO-LUMO gap energy are 0.013 eV, 0.263 eV, 0.025 eV, 0.131 eV for **2a-2d** in HF and 0.066 eV, 0.272 eV, 0.076 eV, 0.143 eV for **2a-2d** in B3LYP.

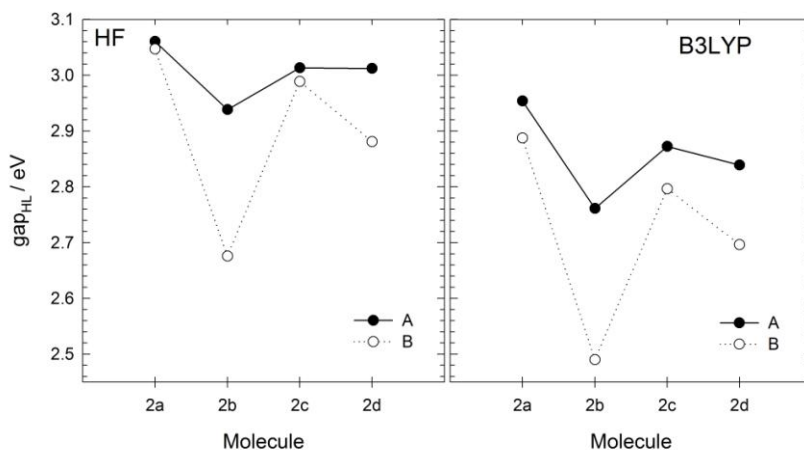


Figure 5. HOMO-LUMO energy gap of **A** and **B** for **2a-2d** with HF and B3LYP

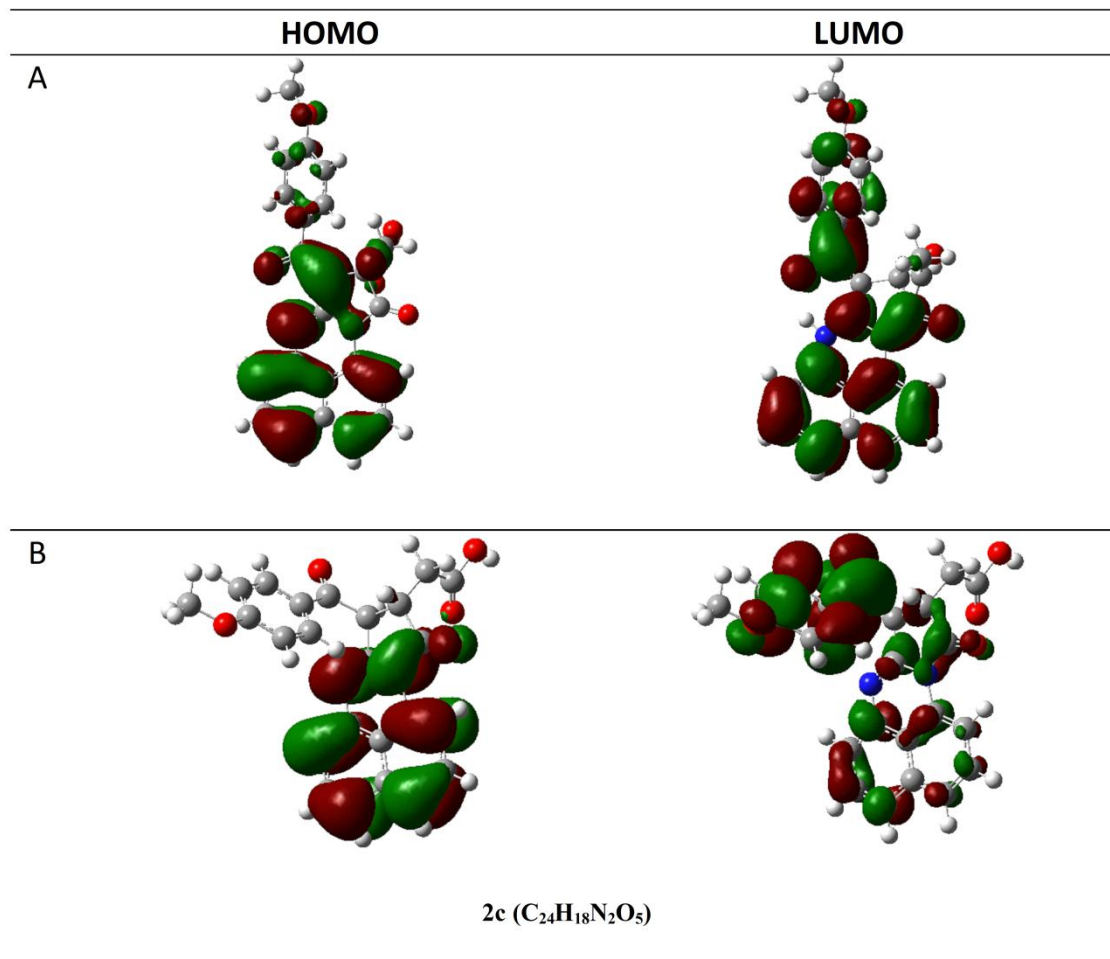


Figure 6. HOMO and LUMO clouds of **A** and **B** for **2c** with B3LYP/6-311++G(d,p)

Moreover, the vibrational frequencies have also been determined. The results are given in Tables S1-4. The vibrational frequencies were calculated for **2(a-d) A** and **2(a-d) B** by using different level of theories. In addition to the predicted frequencies, scaled frequency values and IR intensities are also determined.

The obtained frequency spectra for **2c A** and **2c B** are obtained by HF and DFT/B3LYP methods with 6-311++G(d,p) basis set and experimental data are demonstrated in Figure 7. The R^2 values of the experimental and calculated vibrational frequencies for **2c A** and **2c B** are given in the graphs presented in Figure 8. The highest value of R^2 (0.9998) is found for **2cA** with B3LYP/6-311++G(d,p).

The findings showed that DFT/B3LYP is more-closer to the experimental results. The computational findings showed that the structural stability of **2(a-d)** for tautomer **A** is more than tautomer **B**. It means that the **2(a-d) A** type molecules should be observed more than the tautomer **B** of **2(a-d)** in the product concentrations.

The electronic absorption spectra of the title compounds, which is shown in Figure 9, is taken from a 1.000×10^{-5} M solution prepared by dissolving **2a-d** in DMF solvent. Typically, the electronic absorption spectra of perimidine system consists of two highly intense broad bands with maxima at approx. 230 and 330 nm, which are related to the electronic transitions within naphthalene ring and the transfer of the electron pair of the nitrogen to the antibonding π orbital of the naphthalene, respectively [6]. Frequently, the third low intense absorption related to charge-transfer between the naphthalene ring (π -donor) and hetero-cycle (π -acceptor) is also manifested as a shoulder at 400 nm but its position may vary depending on the substituting group [6,18]. UV-Vis spectrum of **2a-d** was quite typical for

perimidine framework showing the main absorption between 262-265 and 332-344 nm with long-wave shoulder between 355-367 nm. As shown in Figure 9, The HF and B3LYP computations give the UV values agreeing the experimental results.

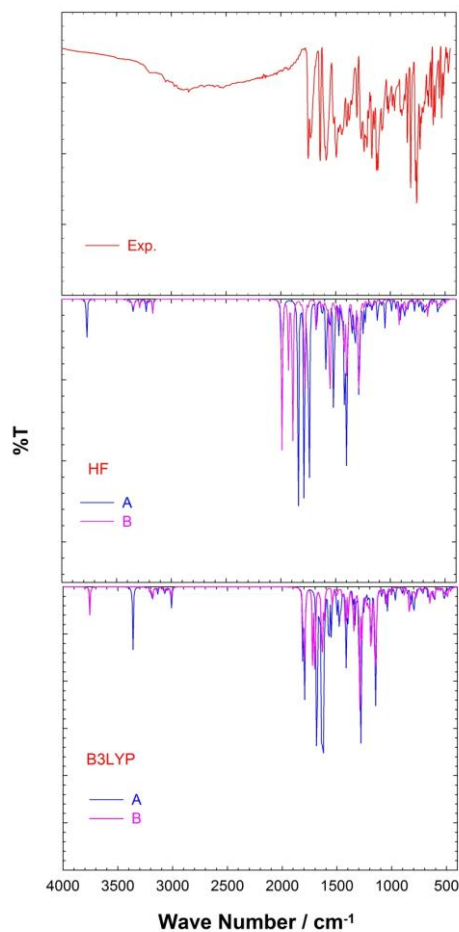


Figure 7. The comparison of the experimental and the theoretical vibrational frequencies of **2c**

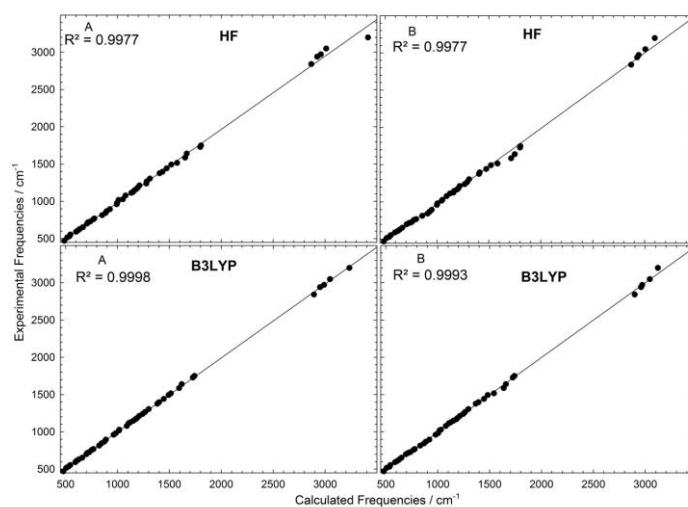


Figure 8. Correlation graphic of experimental and theoretical frequencies of **2c A** and **2c B**

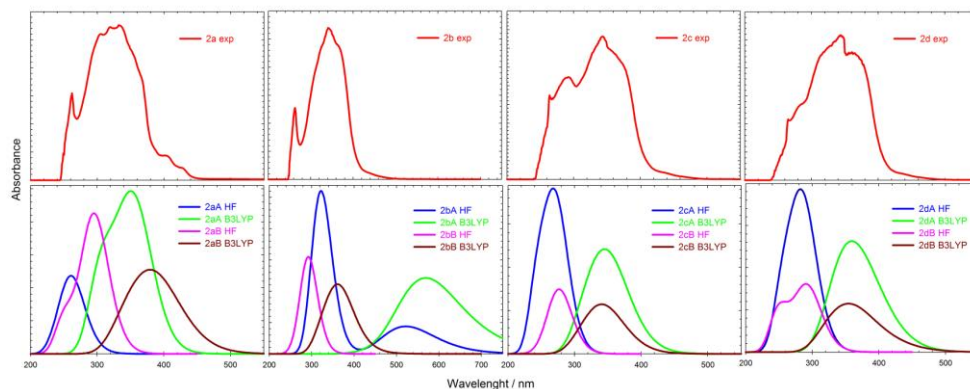


Figure 9. Experimental and theoretical UV-Vis spectra of compound **2a-d**

4. Conclusions

In conclusion, some pyrroloperimidine compounds have been studied by experimental and theoretical approaches. Firstly, we have synthesized and characterized a novel pyrrolo[1,2-a]perimidin-10-ones from HKAs. Elemental analysis, IR, ^1H NMR, ^{13}C NMR and UV techniques were used for characterization. When the structures are identified, especially, examining NMR spectra of these compounds, it is seen that they have two tautomers including enamine and imine form. Experimental data indicate that the enamine form is more than imine form in DMSO- d_6 .

Later, the HF and DFT/B3LYP calculations with 6-311++G(d,p) basis sets have been systematically used to carry out a detailed study on the stable minimum structures of pyrrolo[1,2-a]perimidin-10-ones. We showed that the DFT/B3LYP calculation with 6-311++G(d,p) is more suitable one to describe whole considered structural geometry. As a result, it was found out that the energy of tautomer A was more stable than tautomer B, which supports and confirms the experimental data and findings.

Acknowledgements

The authors would like to thank the Scientific Research Projects Office of Bozok University for financial support (Project No: 2012 FBE/T-01)

References

- [1] Ramsden, W.D.; Valente, L.F.; Bernard, L.S. US Patent 6348592 (2002) Method of making dihydroperimidine squaraine compounds.
- [2] Malherbe, R.F. US Patent 4389321 (1983) 2,3-Dihydroperimidines as antioxidants for lubricants.
- [3] (a) Davis, R.; Tamaoki, N. Novel photochromic spiroheterocyclic molecules via oxidation of 1,8-diaminonaphthalene. *Org. Lett.* **2005**, *7*, 1461–1464; (b) Davis, R.; Tamaoki, N. Modulation of unconventional fluorescence of novel photochromic perimidine spirodimers. *Chem. Eur. J.* **2007**, *13*, 626–631.
- [4] Goswami, S.; Sen, D.; Das, N. K. A New Highly Selective, Ratiometric and Colorimetric Fluorescence Sensor for Cu^{2+} with a Remarkable Red Shift in Absorption and Emission Spectra Based on Internal Charge Transfer. *Org. Lett.* **2010**, *12*, 856–859.
- [5] (a) Bazinet, P.; Ong, T.G.; O'Brien, J.S.; Lavoie, N.; Bell, E.; Yap, G.P.A.; Korobkov, I.; Richeson, D.S. Design of Sterically Demanding, Electron-Rich Carbene Ligands with the Perimidine Scaffold. *Organometallics* **2007**, *26*, 2885–2895; (b) Alıcı, B.; Özdemir, İ.; Karaaslan, K.; Cetinkaya, E.; Cetinkaya, B. Synthesis and catalytic properties of 1-alkylperimidineruthenium(II) complexes. *J. Mol. Catal. A: Chem.* **2005**, *231*, 261–264.

- [6] (a) Pozharskii, A.F.; Dalnikovskaya, V.V. Perimidines. *Russ. Chem. Rev.* **1981**, *50*, 816–835; (b) Claramunt, R.M.; Dotor, J.; Elguero, J. Structure, reactivity, and synthesis of perimidines and their derivatives (dihydroperimidine and perimidinones). *Ann. Quim.* **1995**, *91*, 151–183; (c) Undheim, K.; Benneche, T. *In Comprehensive Heterocyclic Chemistry II*; Katritzky, A.R.; Rees, C. W.; Scriven, E.F.V., Eds.; Pergamon: Oxford, 1996; Vol. 6, Chapter 2.
- [7] Herbert, J.M.; Woodgate, P.D.; Denny, W.A. Potential antitumor agents. 53. Synthesis, DNA binding properties, and biological activity of perimidines designed as minimal DNA-intercalating agents. *J. Med. Chem.* **1987**, *30*, 2081–2086.
- [8] Bu, X.; Deady, L.W.; Finlay, G.J.; Baguley, B.C.; Denny, W.A. Synthesis and cytotoxic activity of 7-oxo-7H-dibenz[f,ij]isoquinoline and 7-oxo-7H-benzo[e]perimidine derivatives. *J. Med. Chem.* **2001**, *44*, 2004–2014.
- [9] Üngören, Ş.H.; Koca, İ.; Yılmaz, F. Preparation of perinones via a novel multicomponent synthesis of isoindole scaffold. *Tetrahedron*, **2011**, *67*, 5409–5414.
- [10] Koca, İ.; Üngören, Ş.H.; Kıbrız, İ.E.; Yılmaz, F. The synthesis of new pyrrolo[1,2-a]perimidin-10-one dyes via two convenient routes and its characterizations. *Dyes Pigments*, **2012**, *95*, 421–426.
- [11] Farghaly, T.A.; Mahmoud, H.K. Site- and regioselectivity of the reaction of hydrazonoyl chlorides with perimidine ketene aminal. Antimicrobial evaluation of the products. *J. Heterocyclic Chem.*, **2015**, *52*, 86–91.
- [12] Şengül, M.Ş.; Cınaklı, S.; Büyükata and M. Hartree-Fock and Density Functional Theory analysis of N-phenyl-1,2-naphthylamine. *Spectrochim Acta A*, **2013**, *114*, 377–393.
- [13] Büyükata, M.; Güvenç, Z.B. DFT study of Al doped cage B12Hn clusters. *Int. J. Hydrogen Energ.*, **2011**, *36*, 8392–8402.
- [14] Büyükata, M.; Güvenç, Z.B. Density functional study of AlBn clusters for n = 1–14. *J. Alloys Compd.*, **2011**, *509*, 4214–4234.
- [15] Frisch M.J. et al., GAUSSIAN 03, Gaussian Inc., Wallingford, CT, 2004.
- [16] Chemcraft (version 1.6, build 304), 2009. <<http://www.chemcraftprog.com>>.
- [17] Young, D.C.; *Computational Chemistry A Practical Guide for Applying. Techniques to Real-World Problems (Electronics)*, John Wiley and Sons, New York, 2001.
- [18] Pozharskii, A.F.; Kashparov, I.S.; Holls, P.J.; Zaletov, V.G. Heterocyclic analogs of pleiadiene. VI. Electronic properties of perimidine. *Khim. Geterotsykl.*, **1971**, *4*, 543–552.

ACG
publications

© 2016 ACG Publications.